International Journal of Bifurcation and Chaos, Vol. 14, No. 5 (2004) 1601–1624

ON A PARTICULAR FOLIATION ASSOCIATED WITH A POLYNOMIAL FAMILY OF NONINVERTIBLE MAPS OF THE PLANE

LAURA GARDINI
*Istituto di Scienze Economiche, University of Urbino, Italy
gardini@uniurb.it

ILARIA FORONI
University Bicocca, Milano, Italy
ilariaforoni@unimib.it

CHRISTIAN MIRA*
19 rue d'Occitanie, 31130 Quint Fonsegrives, France
c.mira@free.fr

Received February 20, 2003; Revised April 4, 2003

The present work describes a family of polynomial noninvertible maps of the plane shared within two open regions: (i) (denoted by Z_0) each point having no real preimage, and (ii) (denoted by Z_2) each point having two real preimages. The regions Z_0, Z_2 are separated by the critical curve LC, locus of points having two coincident preimages. Z_2 is made up of two sheets (giving rise to a plane foliation) joining on LC, each being associated with a well-defined inverse of the map. The considered maps family is structurally unstable. For a wide choice of the parameter space it generates a singular foliation in the sense that the region Z_2 is separated into two zones, Z_2' and Z_2'', inside which the two preimages do not have the same qualitative behavior. Moreover, the boundary between Z_2' and Z_2'' is made up of points having only one real preimage at finite distance, the second one being at infinity. This situation gives rise to a nonclassical homoclinic bifurcation. The maps of the family have another important feature: their inverses present a denominator which vanish along a line of the plane. This has a great consequence on a chaotic attractor structure, when it exists. The imbedding of the map into a wider structurally stable family, generating regions Z_k ($k = 1, 3$ being the number of real preimages), permits to understand the foliation nature when the imbedding parameter cancels leading to the structurally unstable map.

Keywords: Noninvertible maps; Riemann foliation.

1. Introduction

The object of the paper is to describe the dynamic behavior associated with a family of two-dimensional maps having a particular *Riemann foliation* of the phase plane. The family we consider comes from an applied model (to economic and finance, see [Foroni, 2001; Foroni & Gardini, 2003]. This model is not structurally stable. So an explanation of its nonstandard behavior is obtained by imbedding the map into a larger family, which transforms the foliation into one of standard type.

The two-dimensional noninvertible map family is given by

$$T : \begin{cases} x' = cx(y-a) \\ y' = x^2(b-y) \end{cases} \tag{1}$$

It is of *so-called* "$Z_0 - Z_2$" type, i.e. the plane is divided into two regions: Z_2 a point having two real rank-one preimages, Z_0 a point having no real rank-one preimages [Mira *et al.*, 1994, 1996a, 1996b]. Commonly inside Z_2 the plane can be considered as made up of two sheets: one related to the first preimage, the other related to the second one. The two sheets join at a critical curve LC, locus of points having two coincident preimages on the curve LC_{-1}, $T(LC_{-1}) = LC$. With respect to this common situation described in [Mira *et al.*, 1994, 1996a, 1996b] the map (1) gives rise to a particular organization of the sheets associated with each of the two preimages generated by the map. So for $c > 0$ and $b > a > 0$ the resulting plane foliation is singular in the sense that the region Z_2 is separated into two zones Z_2' (the $y < 0$ part of Z_2) Z_2'' ($y > 0$) inside which the two preimages do not have the same qualitative behavior. Moreover, the boundary ($y = 0$) between Z_2' and Z_2'' is made up of points having only one real preimage at finite distance, the second one being at infinity. On the line ($x = 0$) the Jacobian determinant of T vanishes, but its image reduces to a single point (the fixed point $O = (0, 0)$), and we shall see that it is a degenerate focal point of the inverses of T. In the region Z_2'' the two distinct preimages are separated by the line $x = 0$ in which the Jacobian determinant is vanishing.

The imbedding of the map into a wider structurally stable family T_ε, generating regions Z_k ($k = 1, 3$ being the number of real preimages), permits to understand the foliation nature (i.e. the sheets structure of the plane) when the imbedding parameter cancels leading to the structurally unstable map.

The plan of our work is as follows. Section 2 describes some peculiar properties of the map T, their dependance on the parameters a, b and c is considered in subsections. In particular, Sec. 2.1 ($c > 0$ and $b > a > 0$) illustrates the route giving rise to chaotic attractor, by crossing through the first homoclinic bifurcation of the saddle fixed point O. The existence here of a line mapped into a point is associated with a vanishing denominator of the two inverses of the map, which often leads to specific bifurcation cases for a chaotic attractor [Bischi *et al.*, 1999]. Section 3 is devoted to the imbedding of T into a wider family T_ε (ε being the imbedding parameter) generating regions Z_k ($k = 1, 3$). The evolution of the foliation when $\varepsilon \to 0$ permits to identify the sheets organization of the plane at the limit $\varepsilon = 0$. The persistence of the homoclinic bifurcation of the saddle fixed point in the perturbed map T_ε is discussed in Sec. 3.1.

2. Properties of the Family T

2.1. *Some general properties*

In Sec. 2 we describe some features (sometimes very particular) of the two-dimensional map T given in (1). In the next subsection we shall remark on the dynamic behavior of T when the parameter c has positive values, and $b > a > 0$. In Sec. 2.2 we shall see the case $c > o$ and $0 < b < a$ while in Sec. 2.3 the case $a = b$. The case $c < 0$ is considered in Sec. 2.4. Let us describe here some properties which hold in all the cases except for $a = b$.

It is immediate to see that the origin $O = (0, 0)$ is a fixed point of T (not unique as we shall see below), and that the whole line $x = 0$ is mapped into the origin in one iteration. As evidenced in the paper [Bischi *et al.*, 1999], the existence of a line which is mapped into one point denotes the existence of a vanishing denominator in at least one of the inverses of the map. In fact, looking for the preimages of a point (x', y'), we have $y = (x'/cx) + a$ where x is the solution of the following equation

$$c(b-a)x^2 - x'x - cy' = 0 \tag{2}$$

so that we may have no solution or two distinct solutions, called rank-one preimages of (x', y'), given by

$$T_1^{-1}(x', y') : \begin{cases} x = \dfrac{x' - \sqrt{x'^2 + 4c^2y'(b-a)}}{2c(b-a)} \\ y = \dfrac{2(b-a)x'}{x' - \sqrt{x'^2 + 4c^2y'(b-a)}} + a \end{cases} \qquad T_2^{-1}(x', y') : \begin{cases} x = \dfrac{x' + \sqrt{x'^2 + 4c^2y'(b-a)}}{2c(b-a)} \\ y = \dfrac{2(b-a)x'}{x' + \sqrt{x'^2 + 4c^2y'(b-a)}} + a \end{cases} \tag{3}$$

which exist when $x'^2 + 4c^2y'(b-a) > 0$. Thus we have the following two regions, which characterize the

foliation of the plane:

$$Z_0 = \{(x,y) \in \mathbb{R}^2 | x^2 + 4c^2 y(b-a) < 0\} \tag{4}$$

$$Z_2' = \{(x,y) \in \mathbb{R}^2 | x^2 + 4c^2 y(b-a) > 0\,, y < 0\}$$

$$Z_2'' = \{(x,y) \in \mathbb{R}^2 | x^2 + 4c^2 y(b-a) > 0\,, y > 0\} \tag{5}$$

The boundary $y = 0$ separating the two regions Z_2' and Z_2'' is particular because its points have only one of the two distinct rank-one preimages at finite distance. Indeed a point belonging to $y = 0$ with $x > 0$ is such that $T_1^{-1}(x', 0) = (0, \pm\infty)$ and $T_2^{-1}(x', 0) = (x'/c(b-a), b)$ which belongs to the line $y = b$, while if $x < 0$ then $T_1^{-1}(x', 0) = (x'/c(b-a), b)$ belongs to the line $y = b$ and $T_2^{-1}(x', 0) = (0, \pm\infty)$. Clearly, also from the relation given in (2) we have that the inverses of a point with $x' \neq 0$ and $y' = 0$ are $(0, \pm\infty)$ and $(x'/c(b-a), b)$. Thus the x-axis $y = 0$ behaves as a particular set $\tilde{Z}_1$, the points of which have only one real preimage at finite distance.

The boundary separating the two regions Z_0 and Z_2' is the classical critical curve LC defined by:

$$LC : y = \frac{1}{4c^2(b-a)}\, x^2 \tag{6}$$

Each point belonging to LC, except the origin, has two merging preimages on the locus LC_{-1}, which necessarily is a set of points in which the Jacobian determinant of T vanishes. In fact, from (3) we have immediately that the locus of merging preimages has the equation

$$LC_{-1} : y = (2b - a) \tag{7}$$

and $T(LC_{-1}) = LC$. On the other hand, the Jacobian determinant of T is given by:

$$\det J(x,y) = cx^2(y - (2b - a))$$

thus the Jacobian determinant vanishes on LC_{-1} given in (7) and also on the y-axis $x = 0$. However, as noticed above, this set (the vertical axis) is here a particular singular set, because it is mapped into a single point (the fixed point $O = (0,0)$), and it is associated with the vanishing denominator of at least one of the inverses. In fact, as can be seen from the explicit expressions given in (3) (and already remarked above), the half-axis $x' \geq 0$ and $y' = 0$, (resp. $x' \leq 0$ and $y' = 0$) is a vanishing denominator for the second component of T_1^{-1} (resp. of T_2^{-1}). Reminds that a map having a vanishing denominator possesses a set of points, called the prefocal set, whose preimages are related with a single point called the focal point (for more details refer to the paper [Bischi *et al.*, 1999], see also [Bischi *et al.*, 2001, 2002]. In the present case the inverse $T^{-1} = T_1^{-1} \cup T_2^{-1}$ of T has a vanishing denominator, and so the image of $x = 0$ (the prefocal set) is a point ($x = y = 0$) (the focal point), for the inverse map T^{-1}. Indeed this is the case, i.e. arcs through the origin are mapped by $T_{1,2}^{-1}$ into arcs through the point $(0, a)$ or into arcs issuing from two suitable points of the y-axis (which depend on the chosen arc through O). From the properties of the focal point we have that an arc through the origin has both the two preimages at finite distance, issuing from a point of the prefocal set. In our case we have to consider different arcs through the origin. First consider an arc γ in the following parametric form:

$$x(\tau) = \xi_1 \tau + \xi_2 \tau^2 + \cdots$$

$$y(\tau) = \eta_1 \tau + \eta_2 \tau^2 + \cdots$$

with $\xi_1 \neq 0$ and $\eta_1 \neq 0$, taking the images $T_{1,2}^{-1}(\gamma)$ by using the explicit expression given in (3), and letting $\tau \to 0$, then we get two arcs issuing from the single point $(0, a)$ of the y-axis. The qualitative picture of Fig. 1 shows the preimages of two such arcs, labeled γ and η. Then consider a "parabolic"arc γ given by:

$$x(\tau) = \xi_1 \tau + \xi_2 \tau^2 + \cdots$$

$$y(\tau) = \eta_2 \tau^2 + \cdots$$

with $\xi_1 \neq 0$ and $\eta_2 \neq 0$, and its images $T_{1,2}^{-1}(\gamma)$. When $\tau \to 0$, we get two arcs issuing from two distinct points of the y-axis:

$$\left(0, \frac{2(b-a)\xi_1}{\xi_1 - \sqrt{\xi_1^2 + 4c^2(b-a)\eta_2}} + a\right) \text{ with } T_1^{-1}(\gamma)\,,$$

$$\left(0, \frac{2(b-a)\xi_1}{\xi_1 + \sqrt{\xi_1^2 + 4c^2(b-a)\eta_2}} + a\right) \text{ with } T_2^{-1}(\gamma)\,.$$

Thus varying ξ_1 and η_2, i.e. the curvature of such "parabolic" arcs tangent to $y = 0$ at the origin, the whole y-axis can be obtained, which satisfies the definition of prefocal set of the inverses of T. This property clarifies the geometric structure of the attracting set occurring for particular choices of the parameters, as described in the next subsections.

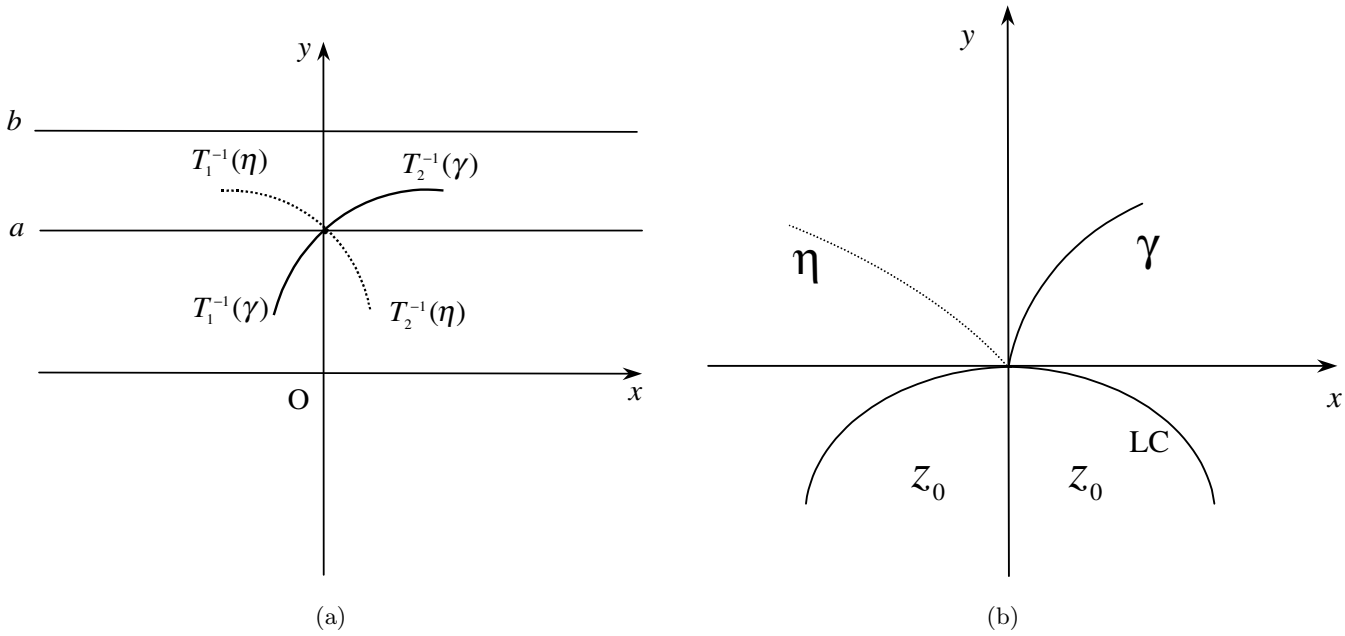

Fig. 1. The preimages of arcs issuing from the origin and belonging to the region Z_2'', as shown in (b), are two arcs issuing from the point $(0, a)$, below the line $y = b$, as shown in (a).

Summarizing, as seen above, the two rank-one preimages of a point $P \in (y = 0)$, $P \neq O$, are one at the point $(0, \pm\infty)$ and the other on the line $y = b$. Thus if P is taken close to the line $(y = 0)$, then one of the two preimages is close to infinity and the other is close to the line $y = b$. Arcs crossing through the origin have two distinct rank-one preimages crossing through the single point $(0, a)$ or through two suitable points of the y-axis (prefocal set of $T_{1,2}^{-1}$).

Besides the elements seen up to now, there is also another peculiarity in the dynamics of the map T: the straight line of equation $y = a$ is mapped into the line $x = 0$ so that its second iterate is the fixed point O, $T^2(\{y = a\}) = (0, 0)$. Clearly, from the property of the line $x = 0$ for T, we can deduce that of the line $y = a$ for the map T^2. That is, $y = a$ is the prefocal set associated with the focal point O for the map T^{-2}. This means that the rank-two preimages of an arc through the origin are arcs which cross the line $y = a$.

The properties described above will have consequences also on the foliation of the plane, as we shall see in the following subsections. It is also worth noting a symmetry property of the map. From $T(-x, y) = (-x', y')$ we have that an invariant set of T is either symmetric with respect to the y-axis, or the symmetric one also exists. So pairs of period-k cycles, k odd or even, the points of which permute in the same way, have this symmetry. This property has consequences on the position of the cycles of T. Looking for the possible fixed points (x^*, y^*) of T we see that besides the origin two more fixed points may exist, when $(ac + 1)/(c(b - a) - 1) > 0$, given as

$$y^* = a + \frac{1}{c}, \quad x^* = \pm\sqrt{\frac{y^*}{b - y^*}} \tag{8}$$

while a period-2 cycle with points $\{P_1, P_2\} = \{(-x_1, y_1), (x_1, y_1)\}$ exists when $(ac - 1)/(c(b-a)+1) > 0$, given by

$$y_1 = a - \frac{1}{c}, \quad x_1 = \pm\sqrt{\frac{y_1}{b - y_1}}\,. \tag{9}$$

2.2. *Case $c > 0$ and $b > a > 0$*

From the analysis of the two inverses given in (3), it is easy to see that in the case $c > 0$, $b > a$ the foliation associated with the map T is very particular. The critical set is the parabola LC belonging to the half-plane $y < 0$, however the portion of plane which is "folded" on LC is only the portion above the line $y = b$, that is, the whole half-plane $y > b$ (which includes LC_{-1}, being $(2b-a) > b$), is mapped (twice) in the region Z_2', as shown in the qualitative drawing of Figs. 1(a) and 1(b). Stated in other words, each point belonging to the region Z_2' has one rank-one preimage belonging to the strip bounded by the

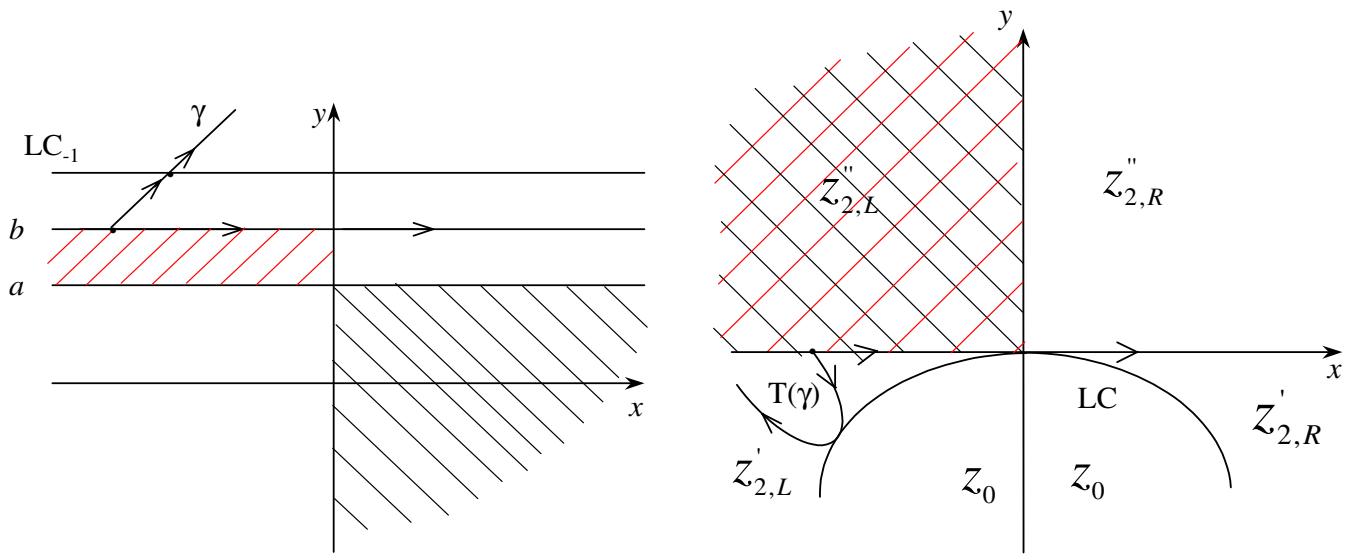

Fig. 2. Structure of the foliation of the map T in the case $c > 0$, $b > a > 0$. The image of an arc γ issuing from the line $y = b$ and crossing LC_{-1} as shown in (a) is folded along LC in an arc $T(\gamma)$ as shown in (b), tangent to LC and belonging to Z'_2.

straight lines $y = b$ and LC_{-1}, while the other rank-one preimage belongs to the half-plane above LC_{-1}, in the region $y > (2b - a)$.

Figure 2 shows that each region Z'_2 and Z''_2 has a symmetric part with respect to the y-axis, labeled left (L) and right (R). Due to the symmetry we can consider only one side, the symmetry giving the behavior on the other side. By analyzing the two preimages given in (3), it is easy to see that any point P belonging to the region $Z''_{2,L}$ has the preimage $T_1^{-1}(P)$ belonging to the left part of the strip bounded by the straight lines $y = a$ and $y = b$, while $T_2^{-1}(P)$ belongs to the right half-plane $x > 0$ below the line $y = a$ (see Fig. 1). Roughly speaking, any point $P \in Z''_{2,L}$ has one of the two preimages on the left, and the other on the right of the vertical axis $x = 0$, one above and one below the straight line $y = a$. Thus we see that these two lines ($x = 0$ and $y = a$) play a special role in the foliation of the plane associated with the map T. In the present case the foliation seems related to the properties of the focal point O for the inverses of T and T^2. From the properties of the focal point we have that an arc through the origin has both the two preimages at finite distance, issuing from a point of the prefocal set. As we have seen in the previous section, in our case these preimages are either issuing from the same point $(0, a)$ (intersection between the two lines $x = 0$ and $y = a$), or issuing from two different points of the axis $x = 0$ (prefocal set of the inverses $T_{1,2}^{-1}$). And $y = a$ is the prefocal set of the focal point O for T^{-2}.

This section shows how the particular foliation is involved in explaining some properties of the dynamic behaviors of the map, associated with the basin boundaries and associated with the attracting sets. At low values of the parameter c the only fixed point is the origin O. It is a stable node for $0 < c < 1/a$ one of its two eigenvalues (or multipliers) always being $S_1 = 0$, the other being $S_2 = -ca$. The value $ac = 1$ ($S_2 = -1$) corresponds to a flip bifurcation giving rise to $c > 1/a$ for the period-2 cycle (9) (stable when ac is not too far from 1), O becoming a saddle. The periodic points, say $P_1 = (-x_1, y_1)$ and $P_2 = (x_1, y_1)$, which are fixed points of the map T^2, give us the opportunity to observe the stable set $W^S(O)$ of the saddle O (which is also related to the basins of T in the case $c < 0$, as we shall see in Sec. 2.4). $W^S(O)$ is the frontier separating the basins $B(P_1)$ and $B(P_2)$ for the map T^2, it is made up of the line $x = 0$ and its rank-n preimages, $n = 1, 2, 3, \ldots$, $W^S(O) = \cup_{n\geq 0} T^{-n}(\{x = 0\})$, $T^{-1}(\{x = 0\}) = (\{y = a\})$.

Figure 3(a) shows these two basins in green and dark gray, and the frontier separating them (i.e. the stable set $W^S(O)$) has arcs in the region Z_0 which are approaching the critical curve LC. The light gray part is the basin $B(\infty)$, set of points having

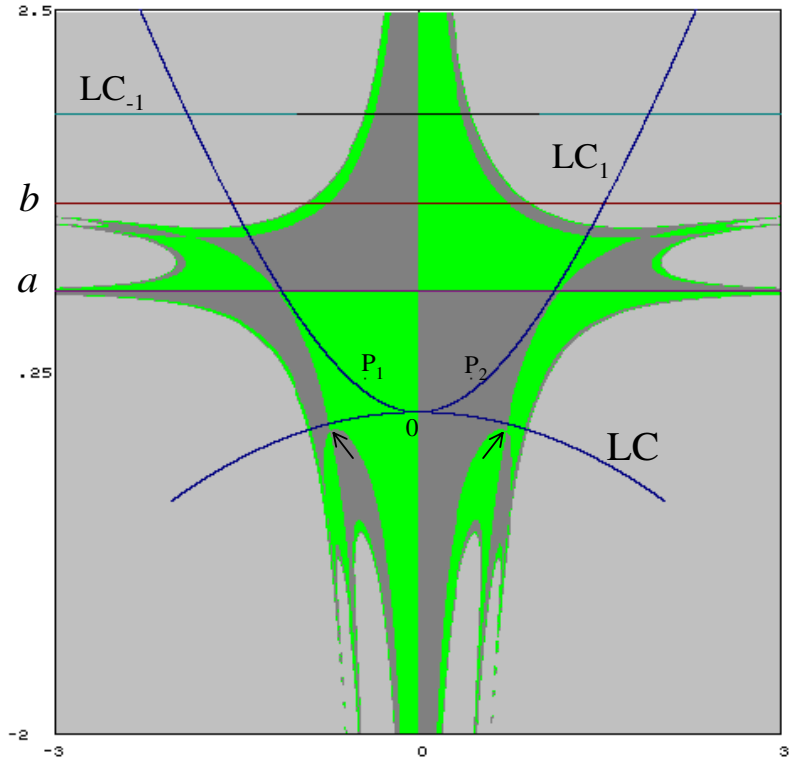

(a)

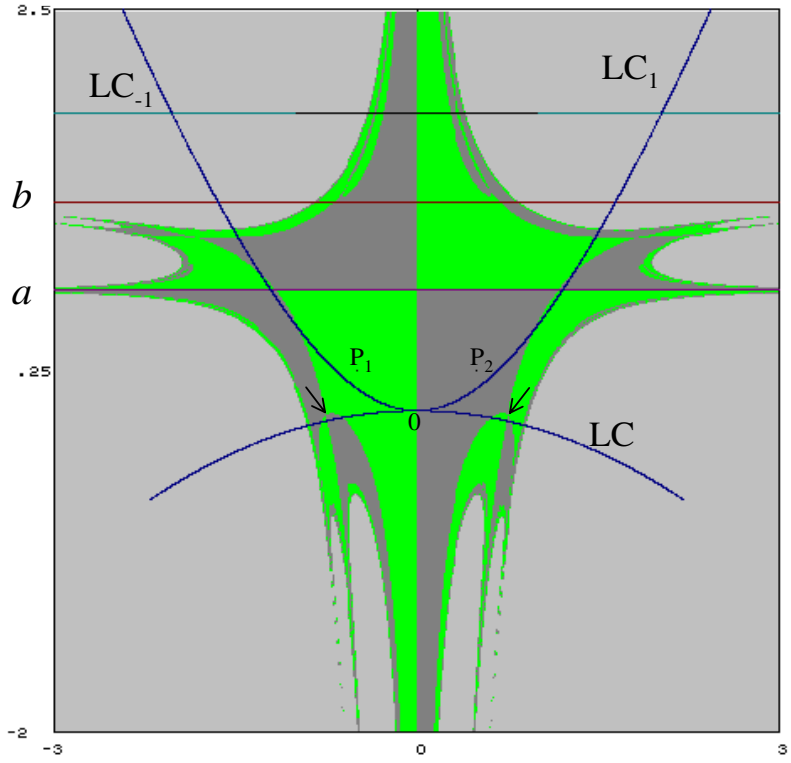

(b)

Fig. 3. Green and dark gray points denote the basins of the points P_1 and P_2 for the map T^2 at $a = 0.75$, $b = 1.3$ and $c = 1.85$ in (a), $c = 2$ in (b). The light gray points belong to the basin $B(\infty)$.

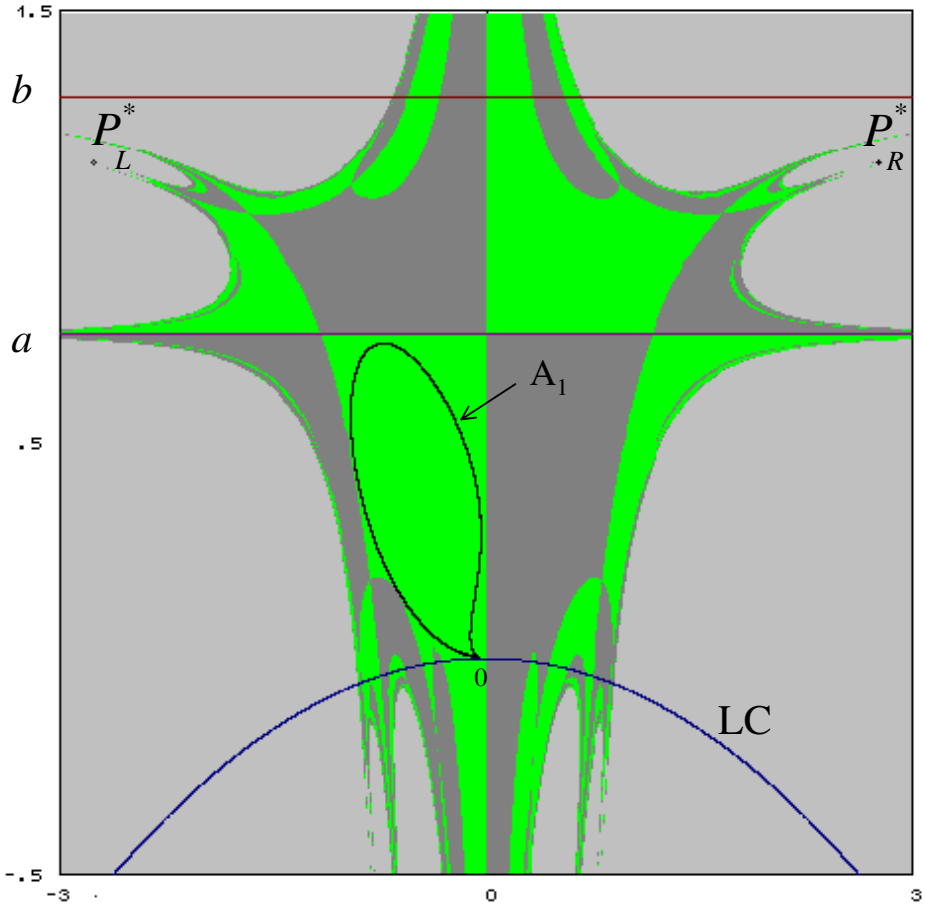

Fig. 4. Green and dark gray points denote the basins of the attractors A_1 and A_2 for the map T^2 at $a = 0.75$, $b = 1.3$ and $c = 2.5$. The light gray points belong to the basin $B(\infty)$, whose boundary includes the fixed points P_L^* and P_R^*.

divergent trajectories. As the parameter c increases (a, b remaining constant), a contact of the frontier with the critical curve LC, followed by a transversal crossing, occurs. This situation causes a qualitative change in the stable set of O and a qualitative change in the structure of the two basins [Mira *et al.*, 1994, 1996a]. It results in the creation of two new portions of the basins [Fig. 3(b)], made up of areas on opposite sides of LC_{-1}, both on the right and on the left of the y-axis (by the symmetry). The frontier $\partial B(\infty)$ is a limit set for $W^S(O)$, and so belongs to its closure. It is asymptotic to the line $y = a$ and to all its preimages of any rank. It also includes the stable set of some cycles. For example, when $c > 1/(b - a)$ two more fixed points of T exist and belong to $\partial B(\infty)$. These fixed points appear (as c increases) due to a *nonstandard* bifurcation occurring at $c = 1/(b - a)$, which involves the improper point (i.e. at infinity) of the line $y = a + (1/c)$ and no other cycle at finite distance. In fact, at this bifurcation value, the two fixed points given in (8), called

$$P_L^* = \left(-\sqrt{\frac{a + \dfrac{1}{c}}{b - \left(a + \dfrac{1}{c}\right)}},\ \left(a + \frac{1}{c}\right) \right),$$
$$P_R^* = \left(\sqrt{\frac{a + \dfrac{1}{c}}{b - \left(a + \dfrac{1}{c}\right)}},\ \left(a + \frac{1}{c}\right) \right) \tag{10}$$

are the points at infinity on the line $y = a + (1/c)$, i.e. $(-\infty, a+(1/c))$ and $(+\infty, a+(1/c))$. This means that for $c = 1/(b - a)$ they constitute the same point on the Poincaré's equator, while after the bifurcation they belong to the frontier $\partial B(\infty)$. Then *we may consider this bifurcation as a pitchfork-bifurcation of a fixed point on the Poincaré equator*. The characteristic polynomial associated with

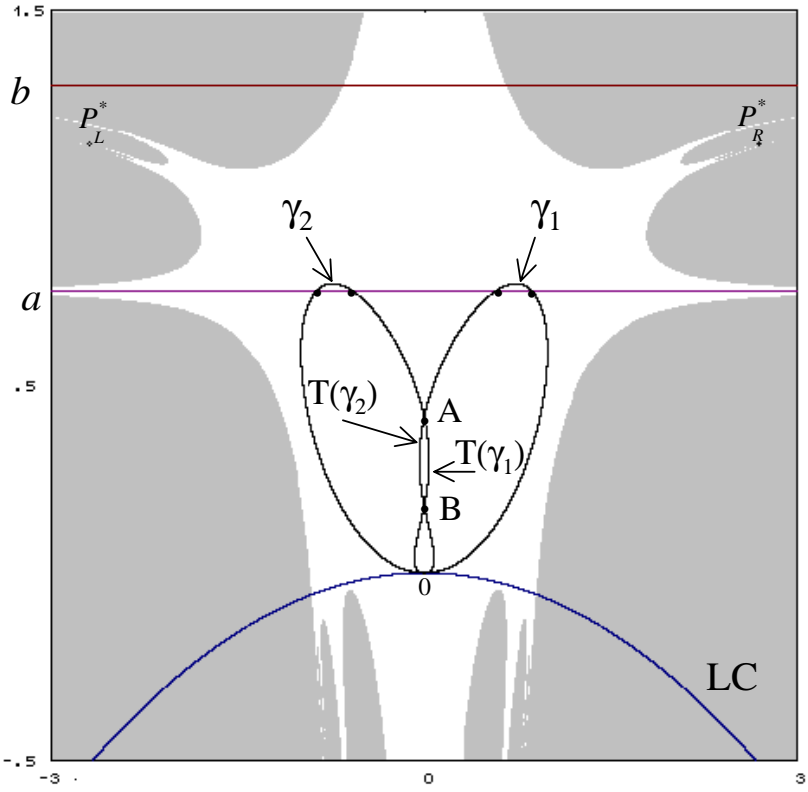

(a)

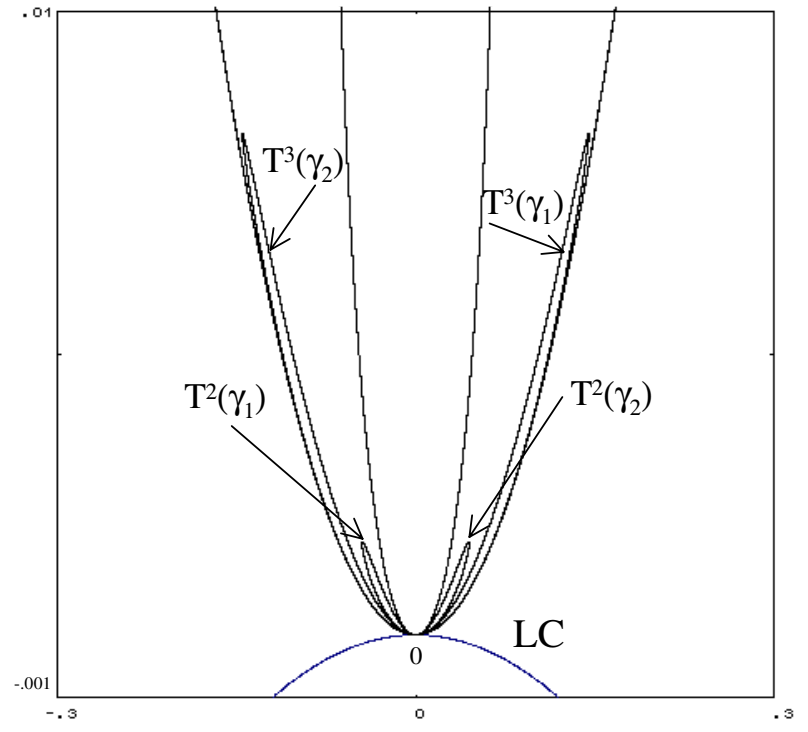

(b)

Fig. 5. Chaotic attractor of T for $a = 0.75$, $b = 1.3$ and $c = 2.545$ in (a). The light gray points belong to the basin $B(\infty)$. (b) Show an enlargement of the region in (a) around the fixed point.

the Jacobian matrices of $J(P_L^*)$ and $J(P_R^*)$ are the same, so that they have the same eigenvalues. At the bifurcation value $c = 1/(b-a)$, roughly speaking, we can say that the two eigenvalues are $S_1 = -\infty$ and $S_2 = 1$, while for $c > 1/(b-a)$, as long as some attracting set at finite distance can be observed, the fixed points P_L^* and P_R^* are two unstable nodes, with $S_1 \ll -1$ and $S_2 > 1$ ($|S_1| > |S_2|$), giving rise to two cusp points of the frontier, and cusps for their increasing rank preimages. These two fixed points on $\partial B(\infty)$ can be seen in Fig. 4.

This figure also shows an attracting set, say $\mathcal{A}_1$, of the map T^2, which with its symmetric (with respect to $x = 0$) part $\mathcal{A}_2$ constitutes a period-2 attractor $\mathcal{A} = \mathcal{A}_1 \cup \mathcal{A}_2$ for T. The attractor $\mathcal{A}$ appears from a Neimark bifurcation undergone by the period-2 cycle $\{P_1, P_2\}$ giving rise to a period-2 invariant closed curve turning into chaotic sets when c increases. Figure 4 shows that for $c = 2.5$ the two symmetric disjoint attractors of T^2 are very close to the stable set $W^S(O)$, boundary separating $B(\mathcal{A}_1)$ and $B(\mathcal{A}_2)$. The two attractors belong to the closure of the unstable set of the origin, $W^U(O)$. A contact between the attractor $\mathcal{A}$ and the basin boundaries $\partial B(\mathcal{A}_1)$ and $\partial B(\mathcal{A}_2)$ corresponds to the appearance of the first homoclinic orbits of the saddle O. After the tangential contact at the bifurcation, a transversal crossing of the stable and unstable sets occurs, $W^S(O) \cap W^U(O) \neq \emptyset$. With the values of a and b used in the figures of this section, this bifurcation occurs at a value c^* such that $c^* \in (2.522, 2.523)$. It is worth noticing that perhaps also for $c < c^*$, c close to c^*, the disjoint attracting sets of T^2 are *weakly chaotic rings* (see [Mira *et al.*, 1996a; Frouzakis *et al.*, 1997]. However, it is certain that the attracting set of T has a chaotic (fractal) structure after the homoclinic bifurcation of O, for $c > c^*$. This is due to the fact that the attracting set necessarily includes infinitely many loops issuing from the origin. An example is shown in Fig. 5.

The images of the sets which seem like arcs in Fig. 5 (but really they are part of a weakly chaotic ring, as it will be clear below) crossing (after the homoclinic bifurcation of O) the straight line $y = a$, denoted by γ_1 and γ_2 in Fig. 5(a), are mapped by T into two symmetric "arcs" issuing from the vertical axis [see the points A and B in Fig. 5(a)], then $T^2(\gamma_i)$ for $i = 1, 2$ are two symmetric "arcs" issuing from the origin, and thus also $T^k(\gamma_i)$ for $i = 1, 2$ and $k > 2$ are two symmetric "arcs" issuing from the origin [see some enlargements in Fig. 5(b)]. And further images of these "arcs" will necessarily cross again the line $y = a$ in other smaller "arcs", whose images will show again loops issuing from the origin, whose images ..., and so on recursively, in a self-similar way. Due to the prefocal property of $x = 0$ related to T^{-1}, mentioned in Sec. 2.1, the images of arcs intersecting the y-axis are arcs with a "parabolic"contact with the x-axis at the focal point O. The inner structure of the chaotic attractor of T can be better observed at a higher value of c, as shown in Fig. 6. The geometric shape of the chaotic attractor at the origin (as shown in Figs. 5 and 6) is clearly explained via the property of the focal point O for the inverses of T^{-1} and T^{-2}, which give, for the forward iterations of T, a particular point (also called *knot point* in [Bischi *et al.*, 2001]).

Up to now we have not commented on the absorbing regions of the map, bounded by arcs of critical curves $LC_k = T^k(LC)$, $k = 1, 2, 3, \ldots$. The attracting sets belong to the strip bounded by the straight lines $y = 0$ and $y = b$, inside which no branch of LC_{-1} or LC exists. However, the critical curve $LC_1 = T(LC)$ belongs to the half-plane $y > 0$ and taking the images of a small segment of LC_{-1} around $x = 0$ a closed *absorbing area* [Mira *et al.*, 1996a] can be obtained, which includes the attracting sets, bounded by an arc of LC_2, as shown in Fig. 7 with the hatched area (the behavior is qualitatively similar at any value of $c > 0$). We can also get the external boundary of a chaotic area, as shown in Fig. 8(a), by using a few images of a very small segment of LC_{-1} around $x = 0$. This external boundary of the chaotic attractor, shown in Fig. 6, is obtained by a few arcs of $LC_2, \ldots, LC_5$. With further images of the same arc we get the shape of the chaotic area in a very few iterations, up to LC_{16}, as shown in Fig. 8(b) (compare this figure with Fig. 6).

It is also clear that increasing c the chaotic area approaches the boundary of its basin, frontier of $B(\infty)$, as shown in Fig. 9, where the value of c is very close to the contact bifurcation, after which only a chaotic repeller survives at finite distance.

2.3. *Case $c > 0$ and $a > b > 0$*

From the analysis of the two inverses given in (3), it is easy to see that in the case $c > 0$ and $a > b > 0$ the foliation of the phase plane is simpler with respect to the previous case. The curve LC_{-1} (line $y = 2b - a$) is below the line $y = b$ which in turn is below the line $y = a$, and the critical curve LC,

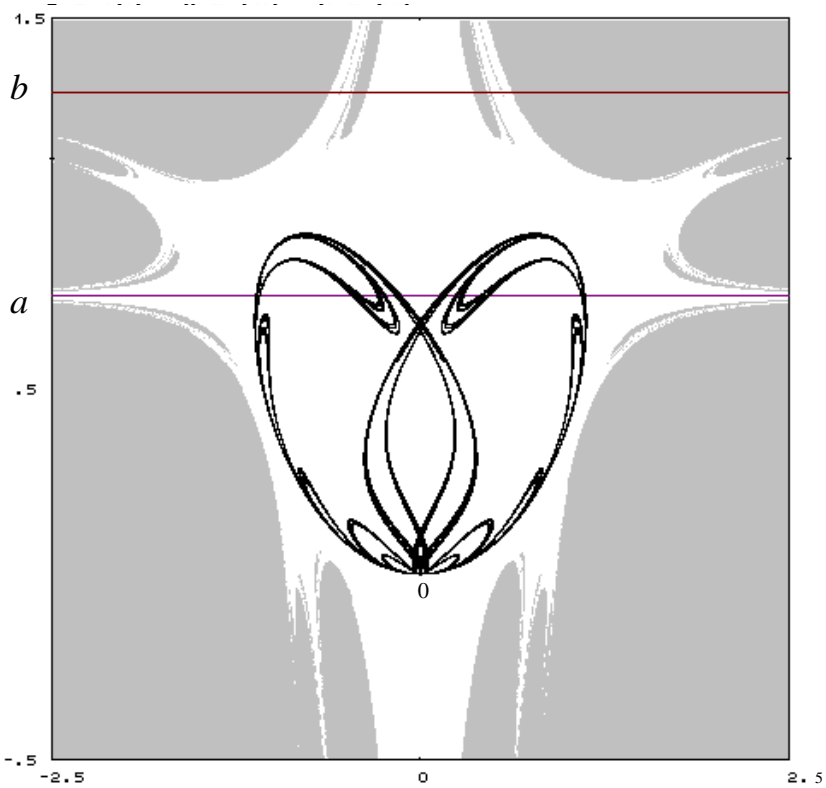

Fig. 6. Chaotic attracting set of the map T for $a = 0.75$, $b = 1.3$ and $c = 2.7$. The light gray points belong to the basin $B(\infty)$.

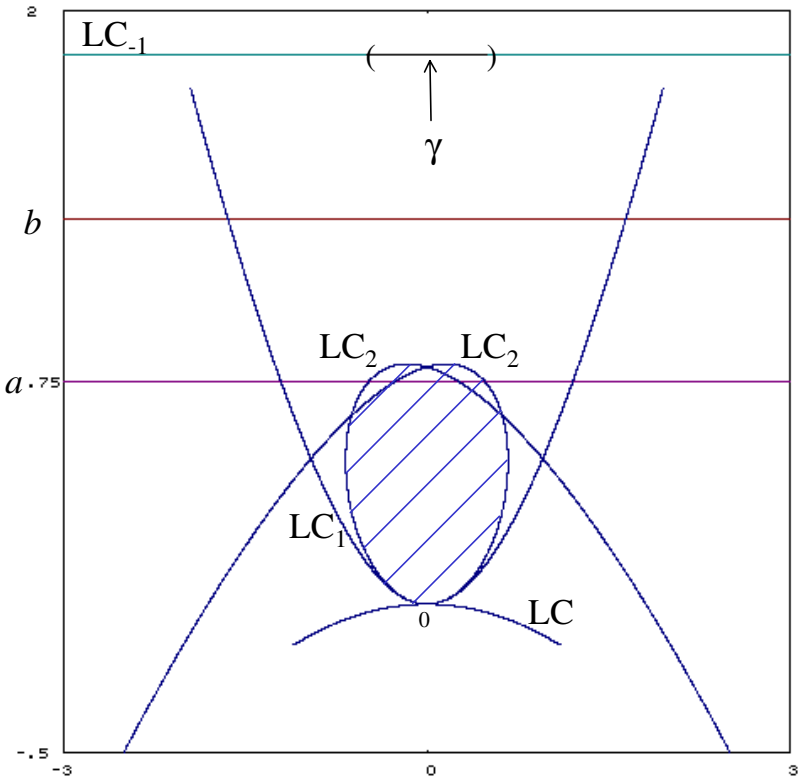

Fig. 7. Forward images of the small arc γ of LC_{-1} for the map T at $a = 0.75$, $b = 1.3$ and $c = 2$. Portions of LC_2 bound an absorbing area.

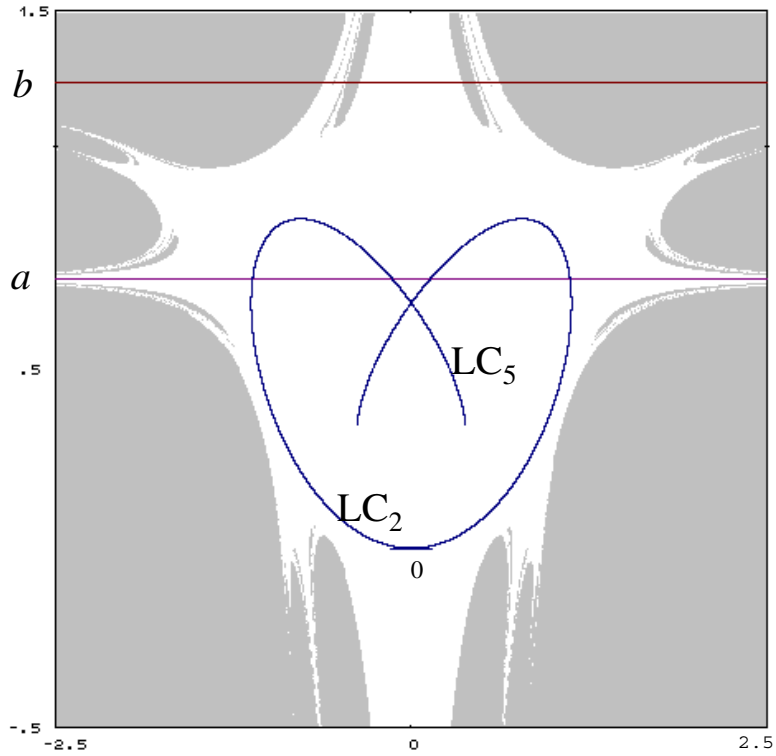

(a)

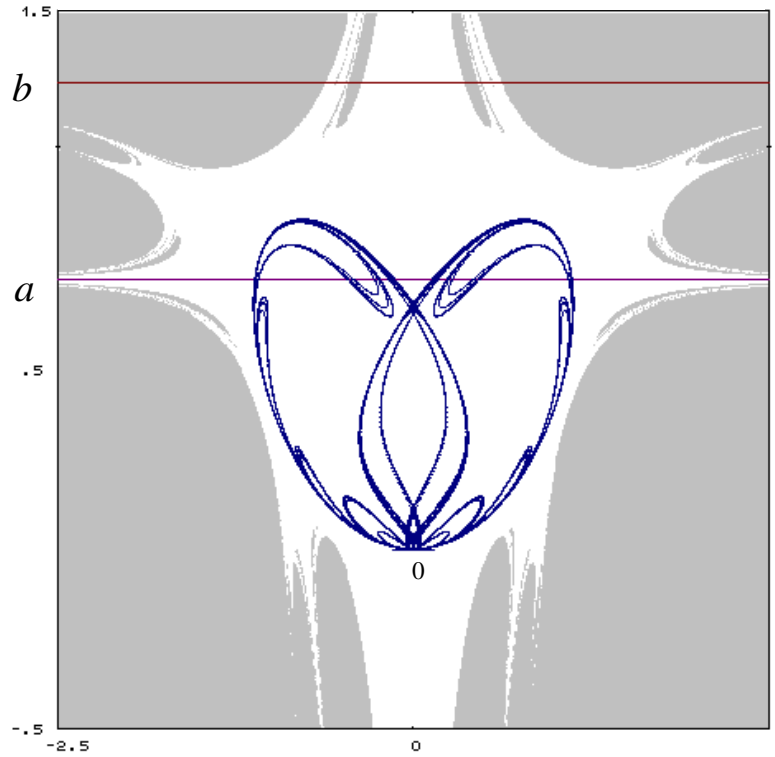

(b)

Fig. 8. (a) The external boundary of the attractor shown in Fig. 6 is obtained with arcs of $LC_2, \ldots, LC_5$, images of a small arc of LC_{-1}. (b) Further images of the same arc of critical curves put in evidence the qualitative shape of the attracting set.

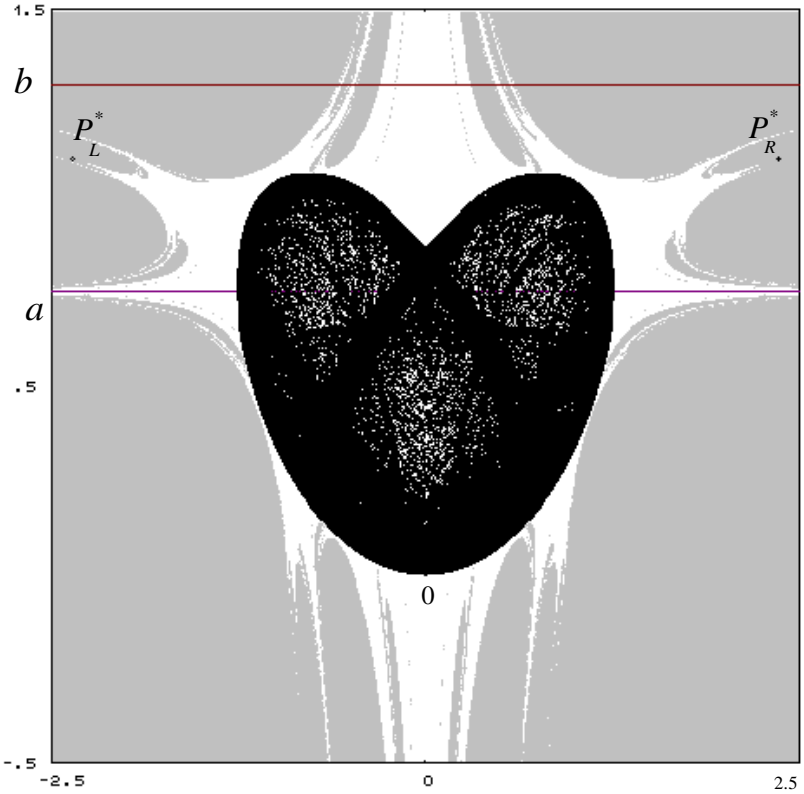

Fig. 9. Chaotic attracting set of the map T for $a = 0.75$, $b = 1.3$ and $c = 2.842$. The light gray points belong to the basin $B(\infty)$.

the parabola given in (6), belongs to the half-plane $y > 0$. The region Z_2'' is the half-plane $y < 0$, while the region Z_2' is the portion of plane between the parabola and the x-axis (see the qualitative picture in Fig. 10). The region Z_2'' still exists which is not crossed by the critical curve LC, and whose preimages are one on the right and another on the left of the line $x = 0$, as well as one above and another below the line $y = a$ (see Fig. 10), but not on the opposite side with respect to LC_{-1}. However, now this region is less interesting from a dynamical point of view (with respect to the case $b > a > 0$) because the attracting sets of T belong to the region Z_2'.

2.4. *Case $c > 0$ and $a = b > 0$*

The transition from the foliation of the plane in the case $b > a$ to that of the case $b < a$ occurs *via* another peculiar families of maps which are obtained from T when $a = b$. In this case the map becomes

$$T : \begin{cases} x' = cx(y - a) \\ y' = -x^2(y - a) \end{cases}$$

The two straight lines $y = a$ and $x = 0$ are mapped into the origin O in one iteration, and no other point can be mapped on the two axes $x = 0$ and $y = 0$. Any other point (x', y') of the plane has a unique preimage given by

$$T^{-1}(x', y') : \begin{cases} x = -\dfrac{cy'}{x'} \\ y = a - \dfrac{(x')^2}{c^2 y'} \end{cases} \tag{11}$$

Thus the map becomes invertible (i.e. with a unique inverse) except for the points on the two axes $x = 0$ and $y = 0$. The two lines $y = a$ and $x = 0$ represent the locus of points in which the Jacobian determinant of T vanishes, being $\det J(T) = cx^2(y - a)$, and also represent the locus of points in which the inverse has a vanishing denominator.

For $ac > 1$ there exists a two-cycle given in (9) (clearly with $a = b$), bifurcated from the origin *via* a flip bifurcation, while for $ac < -1$ there exist two fixed points given in (8), i.e. in (10) (clearly with $a = b$), bifurcated from the origin *via* a pitchfork bifurcation.

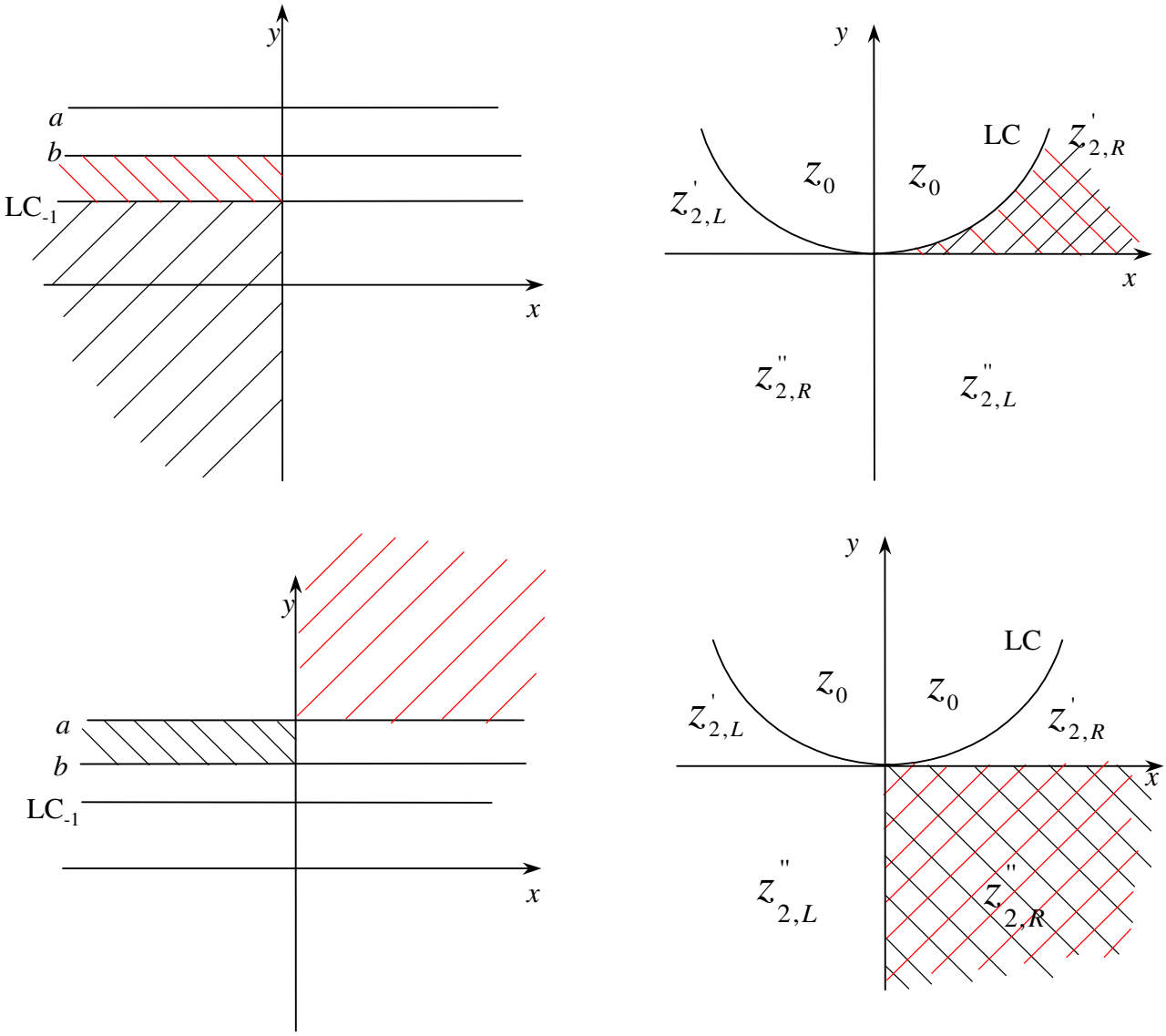

Fig. 10. Critical curves of the map T in the case $c > 0$, $a > b > 0$. The two preimages of a point belonging to Z_2' are on the opposite side with respect to the line LC_{-1}, while the two preimages of a point belonging to Z_2'' are above LC_{-1}, on the opposite side with respect to the line $x = 0$ as well as to the line $y = a$.

We note that the existence of the two lines in the set $S = \{\{y = a\}, \{x = 0\}\}$ mapped into the origin makes the iteration properties of this two-dimensional map T very different with respect to the behavior of the maps with a unique inverse in the whole phase plane. For example, any arc crossing twice this set S is mapped into an arc with a loop in the origin. When the origin O is a saddle, S belongs to the stable set $W^S(O)$. In its turn $W^S(O)$ is given by the preimages of any rank of the line $y = a$. The invariant set constituting the frontier of the set of divergent trajectories $B(\infty)$ is the limit set of $W^S(O)$, boundary between the basins of the two disjoint attractors (of T^2 if $ac > 1$, or of T if $ac < -1$), say $B(\mathcal{A}_1)$ and $B(\mathcal{A}_2)$). See Fig. 11(a), where the attractor is the period-2 cycle of T and the basins shown are those generated by the map T^2. The stable set of the origin is shown in Fig. 11(b), obtained with a few preimages of the line $y = a$.

The peculiar role of the set S becomes evident for the forward iterations of T after the homoclinic bifurcation of O, giving rise to a chaotic attractor which intersects the line $y = a$ in infinitely many arcs with self-similar structure, and consequently loops issuing from the origin. Because of $T(y = a) = O$ we have that the origin is a particular focal point for the inverse T^{-1} and the straight

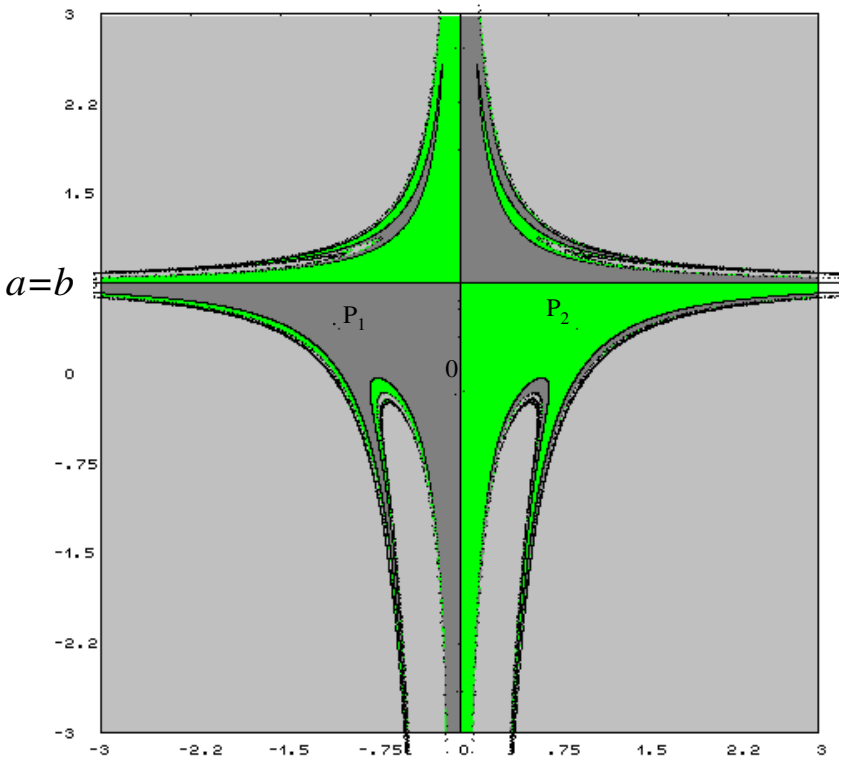

(a)

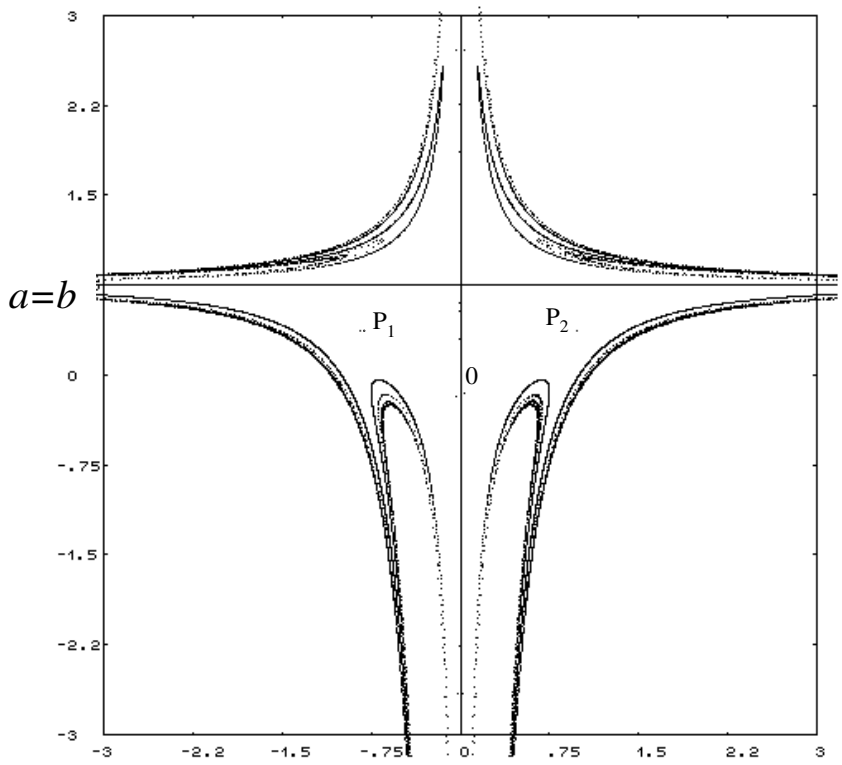

(b)

Fig. 11. Map T in the case $a = b = 0.75$ and $c = 2.6$. (a) Basins of attraction of the points P_1 and P_2 for the map T^2. The light gray points belong to the basin $B(\infty)$. (b) Stable set $W^S(O)$.

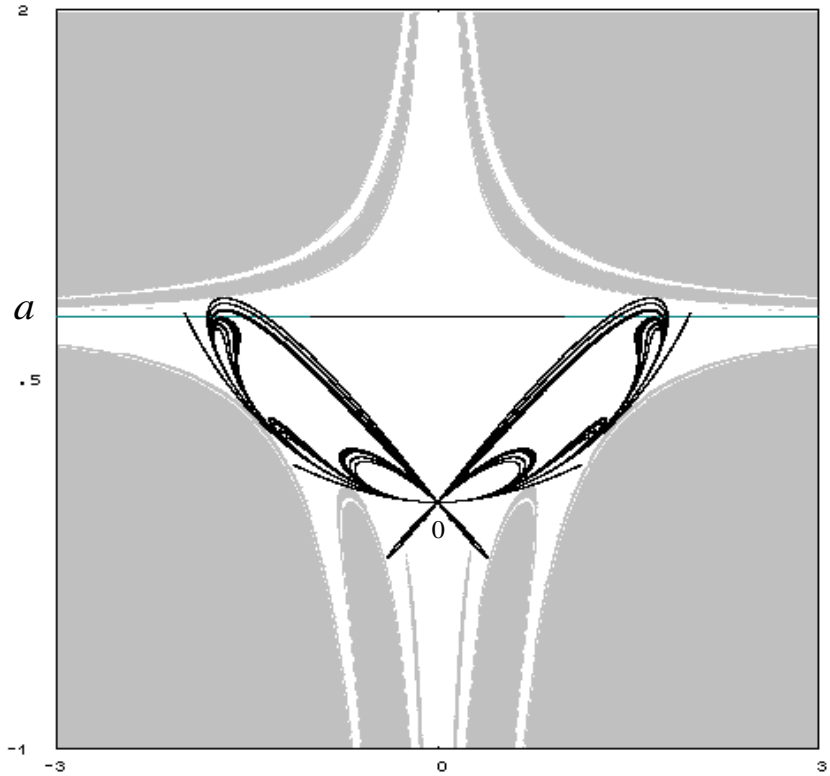

Fig. 12. Chaotic attracting set of the map T for $a = b = 0.75$ and $c = 2.94$. The light gray points belong to the basin $B(\infty)$.

line $y = a$ plays the role of its prefocal set [Bischi *et al.*, 1999, 2001]. This justifies the attractor loops issued from O after crossing through the line $y = a$. An example is shown in Fig. 12, in which the chaotic attractor is close to its final bifurcation, due to a contact with the frontier of its basin.

2.5. *Case* $c < 0$

From the definition of the map $T_c(x, y)$ in (1) where we have evidenced the dependence on the parameter c, it is immediate to see that $T^2_{-c}(x, y) = T^2_c(x, y)$. Thus the case with the parameter c negative comes immediately from that with the parameter c positive. For example, let us consider the case $b > a$. As c decreases from zero the stable fixed point O (attracting node) loses stability at $c = -1/a$ for which a pitchfork bifurcation occurs, giving rise to two stable fixed points, given in (8), i.e. in (10). Then the phase-plane behavior corresponding to the case considered in Fig. 3 with c negative, but with the same absolute value (i.e. $c = -1.85$ and $c = -2$), is exactly the one shown in Fig. 3 (which now represents the basins of T and not of T^2). Similarly the case with $a = 0.75$, $b = 1.3$ and $c = -2.5$ is shown in Fig. 4 where the periodic points on the frontier now belong to a two-cycle, that is, at $c = -1/(b - a)$, a period-2 cycle given in (9) appears from a bifurcation of the point at infinity on the line $y = a-(1/c)$.

3. Perturbed map T_ε

This section considers a map obtained as a perturbation of the map T, showing how the particular foliation associated with the map T, seen in the previous section, may be the result of a bifurcation of another family of maps, given by

$$T_\varepsilon : \begin{cases} x' = cx(y - a) + \varepsilon y \\ y' = x^2(b - y) \end{cases}$$

in which T_0 corresponds to T.

The Jacobian determinant is given by

$$\det(J(T_\varepsilon)) = -x(cx(y - a) + 2(b - y)(cx + \varepsilon))$$

It vanishes on the set LC_{-1} made up of an hyperbola and the vertical axis. The hyperbola

$$LC_{-1,a,b} : \; y = \frac{xc(2b - a) + 2b\varepsilon}{2\varepsilon + cx}$$

is made up of two symmetric branches $LC_{-1,a}$ and $LC_{-1,b}$ [see Fig. 13(a)], with asymptotes $x = -2\varepsilon/c$

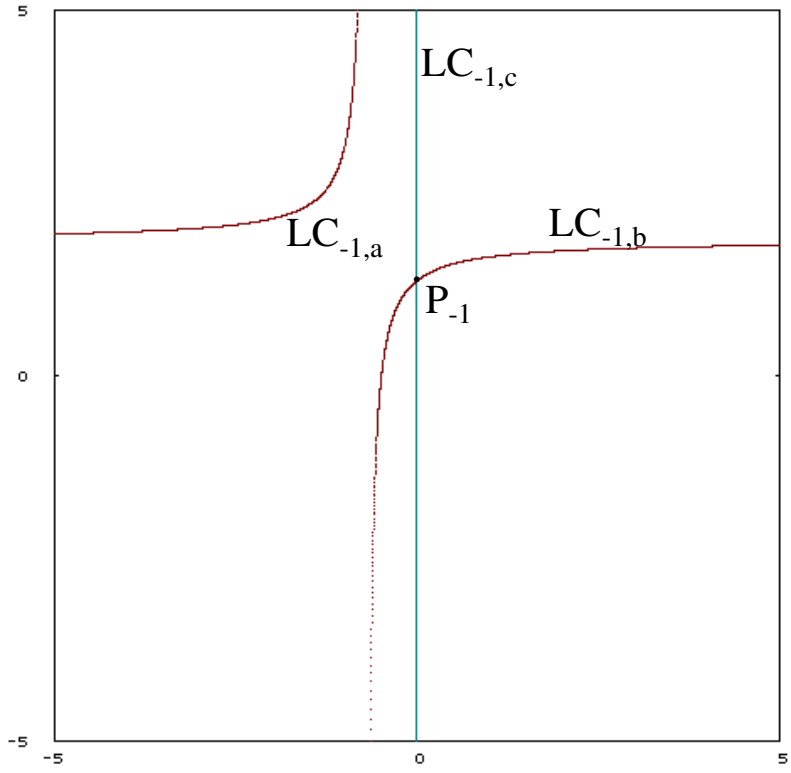

(a)

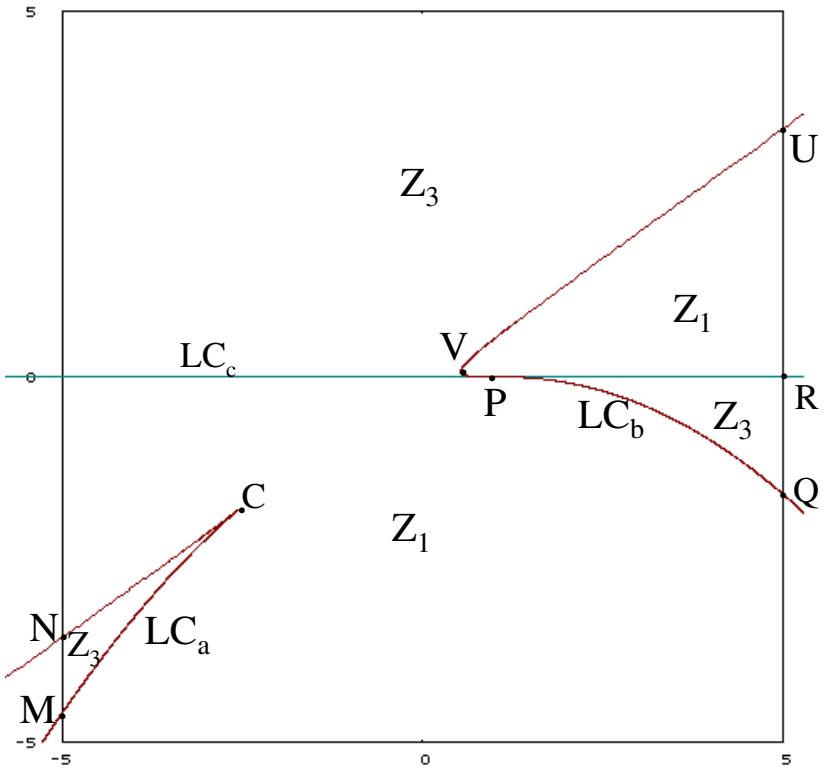

(b)

Fig. 13. Critical curves of the map T_ε for $a = 0.75$, $b = 1.3$, $c = 2$ and $\varepsilon = 0.7$. LC_{-1} in (a), LC in (b).

and $y = (2b - a)$. The third branch is:

$$LC_{-1,c}: \; x = 0\,.$$

The locus LC_{-1} is $LC_{-1} = LC_{-1,a} \cup LC_{-1,b} \cup LC_{-1,c}$. For the sake of simplicity, we only comment the case $c > 0$ and $b > a > 0$ (the other cases are straightforward). The rank-one image of LC_{-1} is LC made up of three branches, $T_\varepsilon(LC_{-1,a}) = LC_a$, $T_\varepsilon(LC_{-1,b}) = LC_b$, and $T_\varepsilon(LC_{-1,b}) = LC_b = (y = 0)$ [see Fig. 13(b)]. These branches of LC separate the phase plane into open regions Z_i, $i = 1, 3$ (as will be explained below), i being the number of distinct rank-one preimages of a point Z_i. Crossing through a branch of LC the number of distinct rank-one preimages changes. The preimages (x, y) of a point (x', y') of the phase plane are not easily computable, depending on the real solutions of the cubic equation:

$$\begin{gathered} c(b-a)x^3 + (\varepsilon b - x')x^2 - cy'x - \varepsilon y' = 0 \\ y = b - \frac{y'}{x^2} \; (x \text{ a solution of the cubic equation}) \end{gathered} \tag{12}$$

Thus the distinct preimages of a point (x', y') inside the open regions Z_1 (or Z_3) are either one (or three). It is easy to verify that whenever a point (x', y') crosses through a branch of LC_{-1} the number of its distinct preimages changes as qualitatively shown in Fig. 13(b) so that, following the notation used in [Gumowski & Mira, 1980] and in [Mira *et al.*, 1996a, 1996b], all these curves belong to the critical set denoted by LC.

The foliation of the phase plane associated with the map T_ε (for $\varepsilon \neq 0$) is qualitatively shown in Fig. 14(a). This figure shows the disposition of the "sheets" (one or three), each one being related to a rank-one preimage of a point $P' = (x', y')$, say $p_i = (r_i, y_i)$. Each sheet is related to one of the real roots of the cubic equation given in (12), denoted as r_i, $i = 1, 2, 3$, $r_1 < r_2 < r_3$ when they are three, while in the case of only one root it may be negative ($r_1 < 0$) or positive ($r_3 > 0$). The branch of critical curve LC denoted by LC_a has a cusp point in C (in which we have $r_1 = r_2 = r_3$) and the two branches issuing from the cusp point are denoted by NC and MC. The branch LC_b has a smooth point in the turning point V. A cusp point exists at the intersection with the other critical branch LC_c at the point P on the x-axis (in which we have $r_1 = r_2 = r_3 = 0$). The two branches issuing from the cusp point are denoted by PR (on the x-axis) and PQ. While the branch PQ of LC_b is associated with the reunion of two sheets belonging to $y < 0$ [see Fig. 14(a)], the other part of LC_b, the arc PVU, is associated with the reunion of two sheets belonging to $y > 0$. Similarly a different role occurs on the critical branch LC_c: the segment PR is associated with the reunion of two sheets belonging to $y < 0$, the other part of LC_c, the segment PT, is associated with the reunion of two sheets belonging to $y > 0$. The regions with a single root are the portion Z_1 belonging to $y < 0$ (in which we have one negative root), and the region Z_1 belonging to $y > 0$, the one bounded by a branch of LC_c (PR) and a branch of LC_b (PVU) (in which we have one positive root).

As the parameter $\varepsilon \to 0$ the branch CN of the critical curve LC_a approaches the branch OT of the critical curve LC_c (for $\varepsilon = 0$ the cusp point C merges with the origin O), while the branch PVU of the critical curve LC_b approaches the branch PR of the critical curve LC_c (for $\varepsilon = 0$ the cusp point P merges with the point V and with the origin O). See Fig. 15(a) obtained with a low value of ε.

For $\varepsilon = 0$ the cubic equation in (12) reduces to

$$x(c(b-a)x^2 - x'x - cy') = 0 \tag{13}$$

so that whichever is the point (x', y'), one root is $x = 0$, and the remaining quadratic equation in (13) is the same as the one given in (2), but the root associated with $x = 0$ is not real (having $y = \infty$). So that the map T_0 loses one root at finite distance at each point of the plane, becoming a map with either two real preimages or zero, and the foliation of the plane (which loses one sheet) is qualitatively shown in Fig. 14(b) and fully explains the particular structure of the map T of type "Z_0, Z_2" considered in the previous section (see Fig. 1).

For $\varepsilon < 0$ the foliation of the phase plane associated with the map T_ε has a structure similar to that existing for $\varepsilon > 0$. The only change is in the geometrical position of the two branches of hyperbola $LC_{-1,a,b}$ and thus of their image $LC_{a,b}$ giving the foliation qualitatively shown in Fig. 15(b). In spite of the position of the critical branches with cusp points the structure of the foliation is clearly similar to that of Figs. 15(a) and 14(a).

The perturbed map T_ε has an increased number of preimages with respect to the map T_0. This may clearly give rise to differences of behaviors in the basins of attraction generated by the two maps, the preimages playing a fundamental role. It is not the case for the structure of the attracting sets which may not be strongly influenced. An example will be shown in the next subsection.

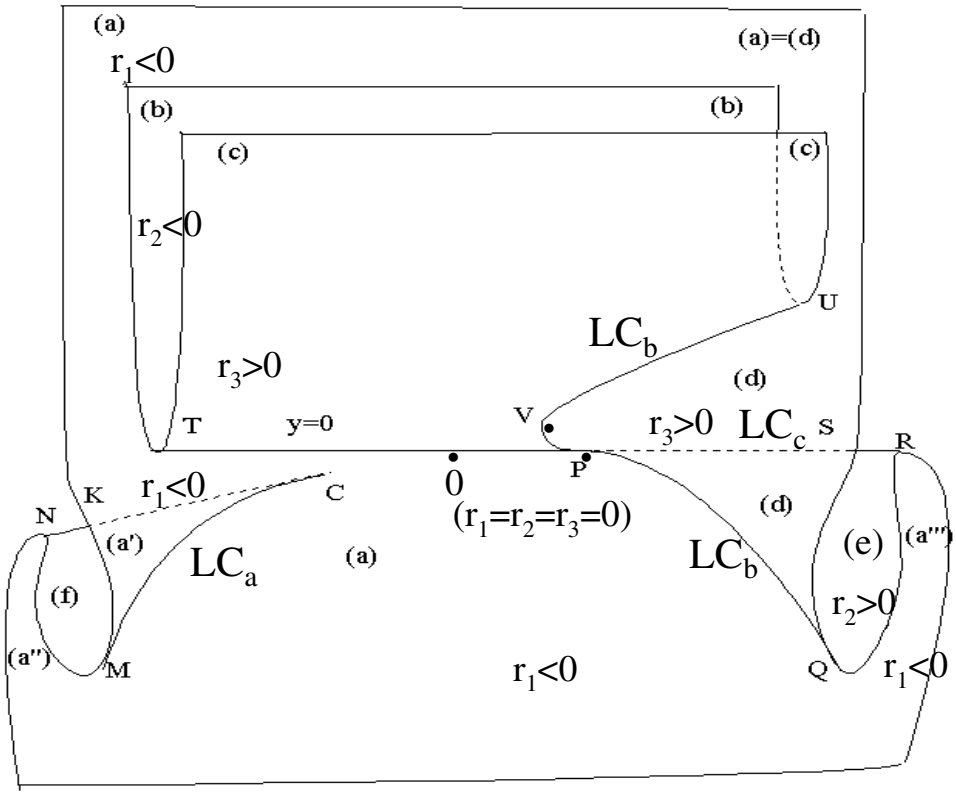

(a)

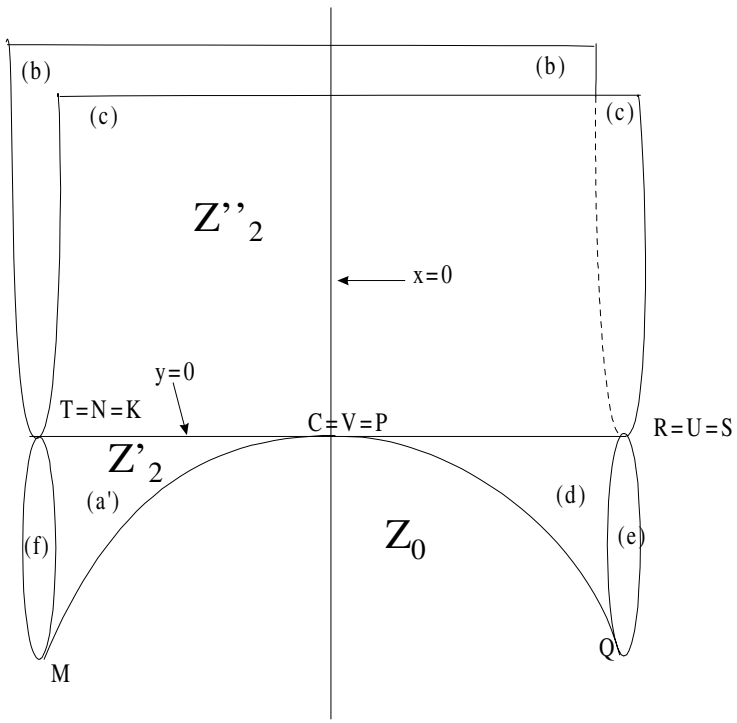

(b)

Fig. 14. Qualitative structure of the *Riemann foliation* of the plane for the map T_ε in the case $c > 0$, $b > a > 0$. For $\varepsilon > 0$ in (a), for $\varepsilon = 0$ in (b).

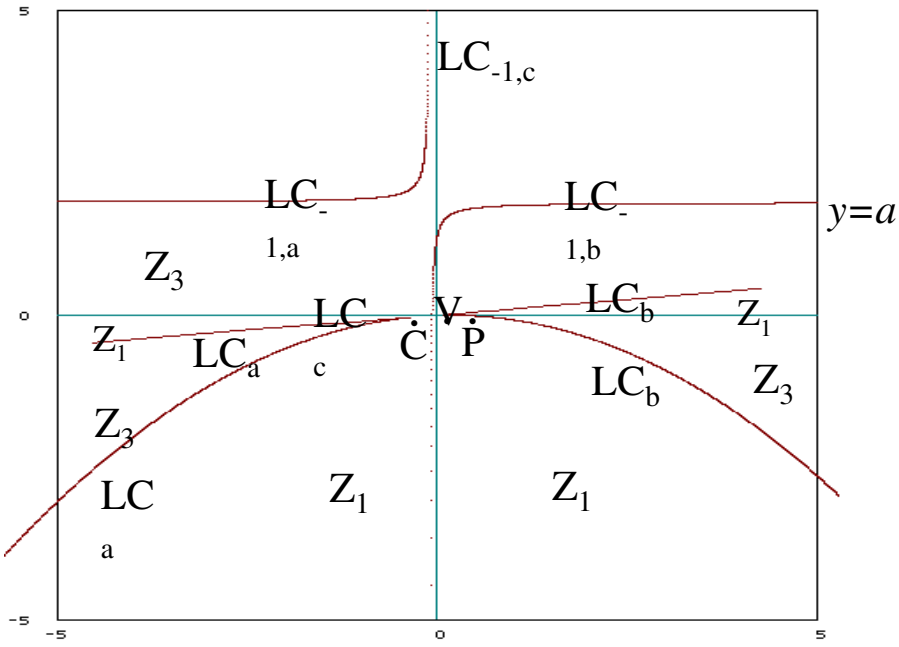

(a)

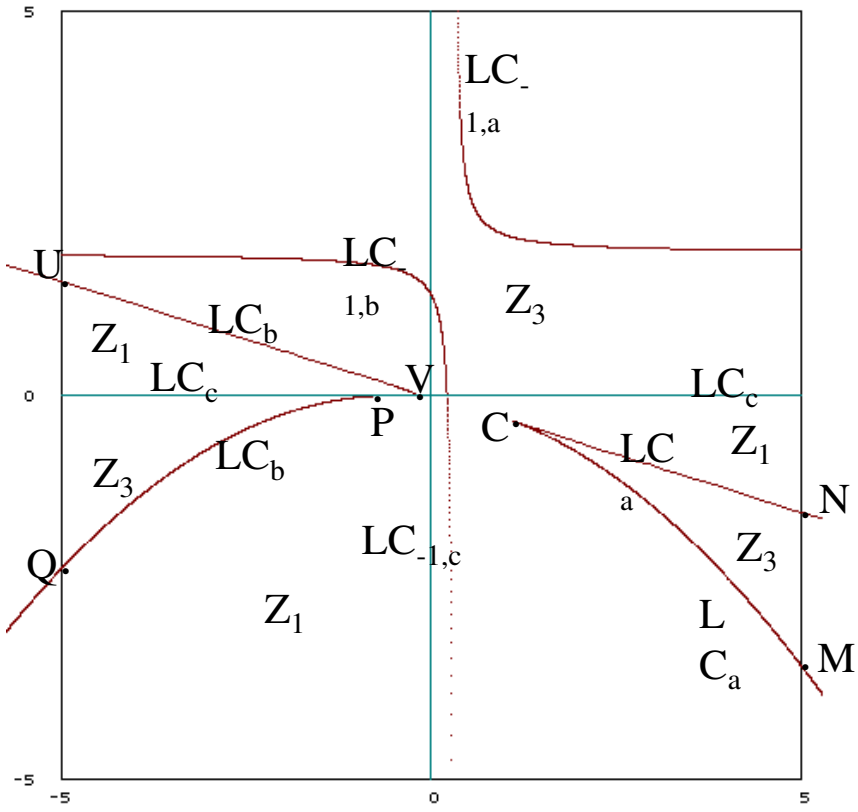

(b)

Fig. 15. Critical curves and zones $Z_1 - Z_3$ for the map T_ε in the case $c > 0$, $b > a > 0$. For $\varepsilon > 0$ in (a), for $\varepsilon < 0$ in (b).

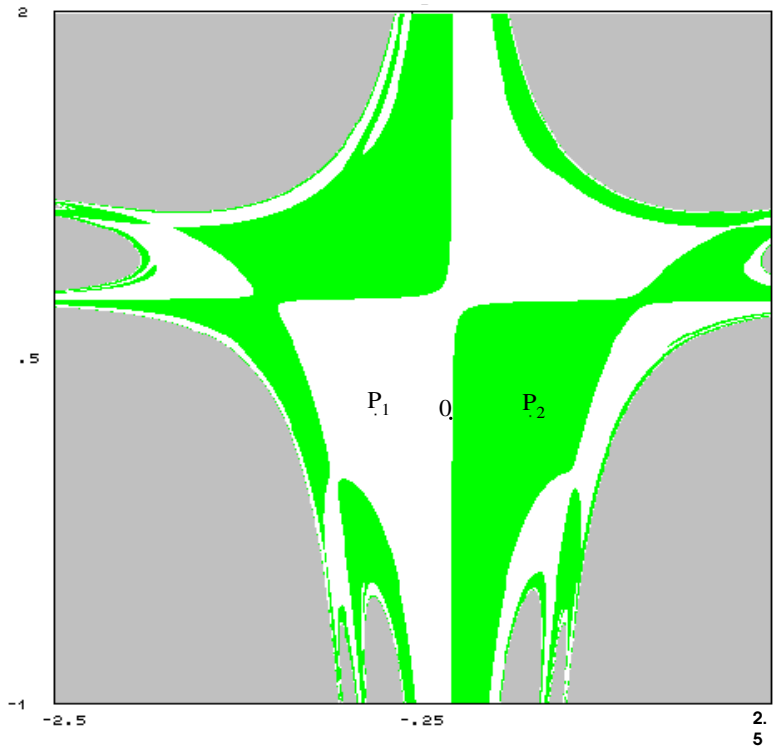

(a)

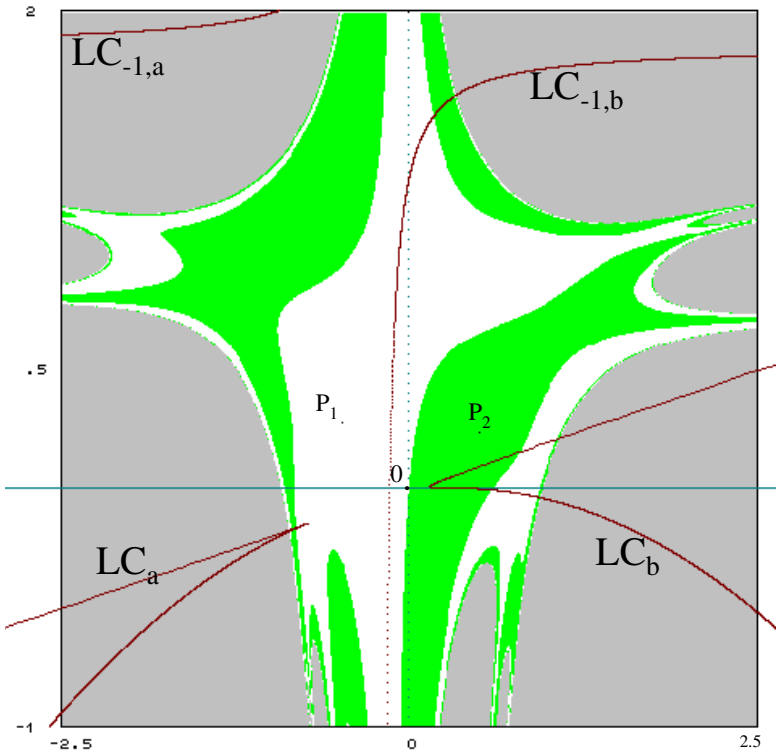

(b)

Fig. 16. Basins of attraction of the points P_1 and P_2 for the map T_ε^2 for $a = 0.75$, $b = 1.3$, $c = 2$ and $\varepsilon = 0.1$ in (a), $\varepsilon = 0.2$ in (b).

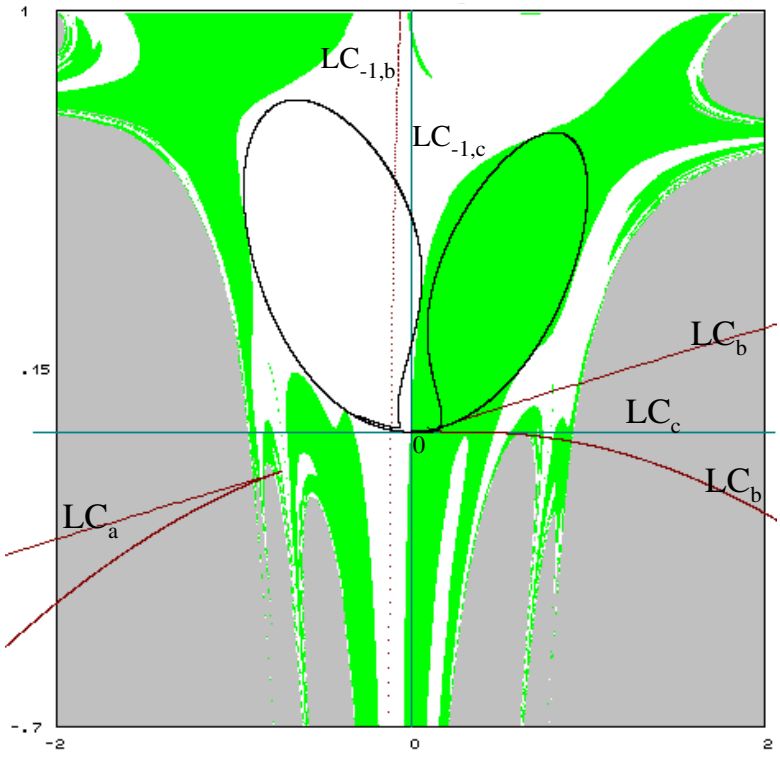

(a)

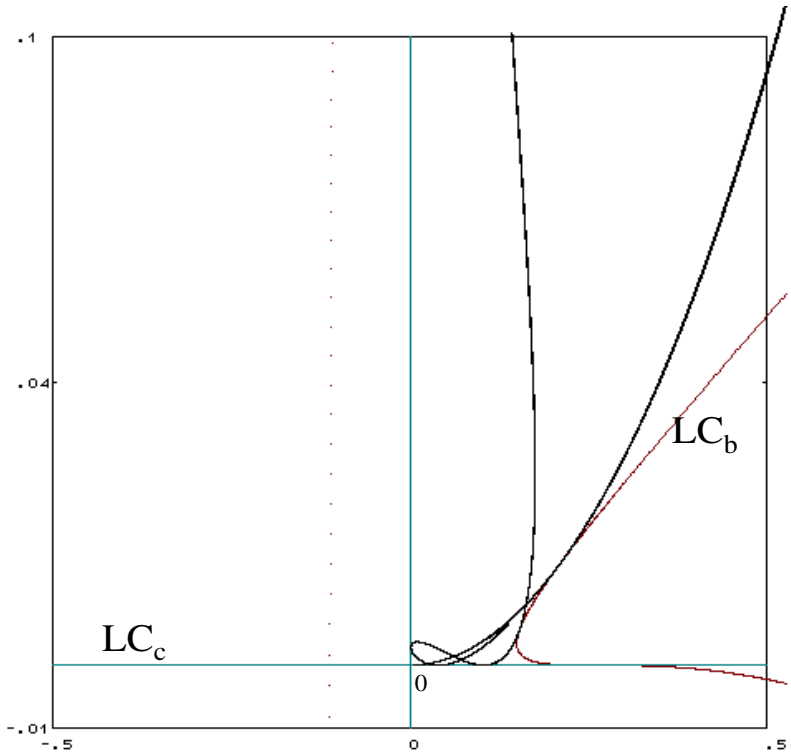

(b)

Fig. 17. Basins of attraction of the chaotic attractors A_1 and A_2 for the map T_ε^2 for $a = 0.75$, $b = 1.3$, $c = 2.52$ and $\varepsilon = 0.2$. (b) Shows an enlargement of the region in (a) around the fixed point.

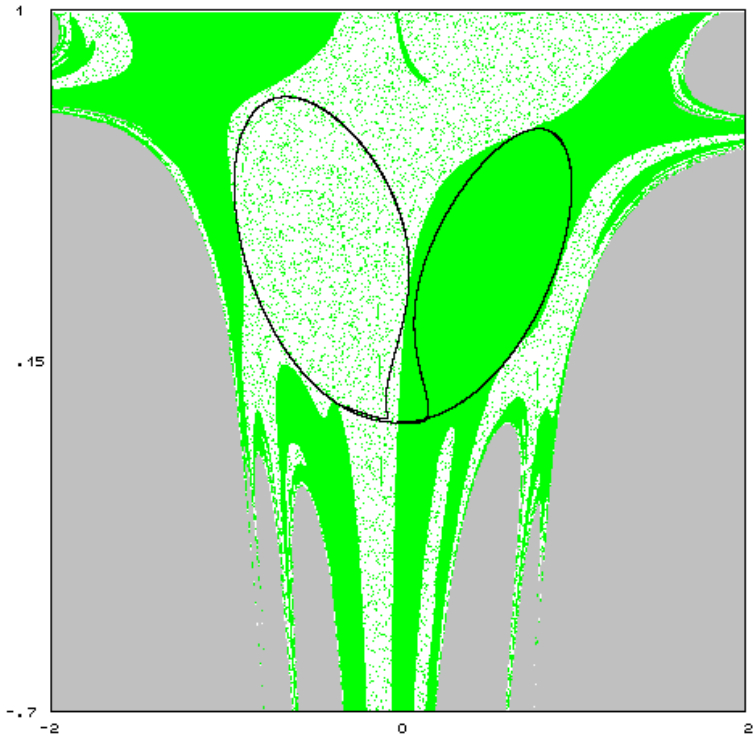

(a)

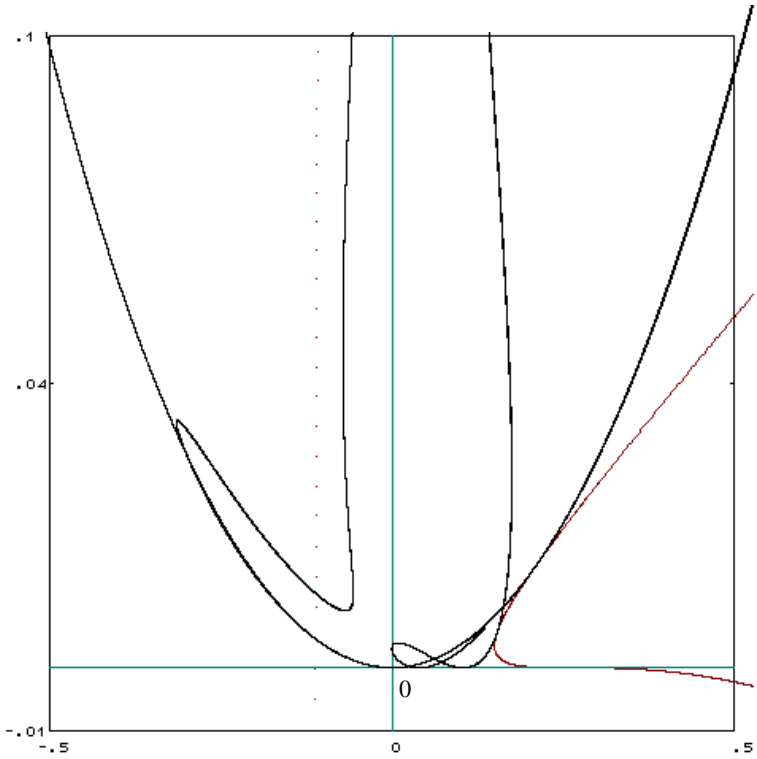

(b)

Fig. 18. Chaotic attracting set of the map T_ε for $a = 0.75$, $b = 1.3$, $c = 2.521$ and $\varepsilon = 0.2$. (a) The green points are those which visit the right side of the attracting set in less than 100 iterations of T_ε. (b) Shows an enlargement of the region in (a) around the fixed point.

3.1. *Some attractors of T_ε*

This subsection gives some examples of the attracting sets and their basins generated by the map T_ε as ε increases from 0, starting from the case already described in Fig. 3. An example of perturbation is shown in Fig. 16(a), where the parameter ε is very small.

The attracting set of T_ε is a cycle of period-2, which corresponds to a couple of fixed points for the map T_ε^2. This gives us the possibility to show the structure of the stable set of the origin O (now a saddle fixed point). This set $W^s(O)$ is the frontier of the two basins (in white and green) in Fig. 16(a). Differently from what occurred in Fig. 3 the local stable set of O is no longer the whole x-axis, and the symmetry is broken. Figure 16(b) shows the same basins for a higher value of ε, the change in the basin structure being more evident. Increasing the parameter c the Neimark-bifurcation of the two-cycle occurs (as expected) and the basins maintain the same qualitative structure. The two disjoint attracting sets (for the map T_ε^2) grow in size approaching the frontier of their basins, as shown in Fig. 17(a). An enlargement of the attracting set on the right is shown in Fig. 17(b), showing that the attracting set is already a *weakly chaotic ring*. The origin O is still a saddle without any homoclinic orbit (as no intersection exists between its stable and unstable sets).

Nevertheless the attracting sets are quite close to their frontier, and as c is further increased the homoclinic bifurcation of O occurs when the attracting sets have a contact with the frontiers. Figure 18(a) shows the attracting set after the homoclinic bifurcation of O. Also for the map T_ε^2 the attracting set is now unique [see the enlargement in Fig. 18(b)]. The basin in Fig. 18(a) is of a unique color (being a unique attracting set), but we have shown the occurrence of the transverse crossing through the stable and unstable sets of O by coloring in green the points which visit the right side of the attracting set in less than 100 iterations of T_ε.

4. Conclusions

The present work has described a family T of polynomial noninvertible maps of the plane, which is structurally unstable. Except for the case in which the parameters a and b are equal, the plane is shared within open regions: Z_0, whose points have no real preimage, while two real preimages exist in the region Z_2. For a wide choice of the parameter space T generates a singular foliation in the sense that the region Z_2 is separated into two zones, Z_2' and Z_2'', inside which the two preimages do not have the same qualitative behavior. Moreover the x-axis, boundary between Z_2' and Z_2'', is made up of points having only one real preimage at finite distance, the second one being at infinity. This situation gives rise to a nonclassical homoclinic bifurcation. We have seen that imbedding the map into a wider structurally stable family, T_ε, we get regions Z_k ($k = 1, 3$ being the number of real preimages) which permits to understand the foliation nature when the imbedding parameter cancels leading to the structurally unstable map.

It is worth emphasizing the essential role, played by the inverse map having a vanishing denominator, on the chaotic attractor structure, as appearing in Figs. 5 and 6. This is due to the fact that the attractor contains the focal point of the inverse (here unique knot because it is a fixed point). Figure 37 of the papers [Bischi *et al.*, 1999, 2003] shows an equivalent situation, but with a focal point which is not fixed, so that its increasing rank images are knot points of the attractor. The "dual situation" occurs when a map itself has vanishing denominators, which leads to lobes of basins at the focal points and their increasing rank preimages [Bischi *et al.*, 1999, 2003].

Acknowledgments

This work has been performed under the activity of the National Research Project "Nonlinear models in economics and finance: complex dynamics, disequilibrium, strategic interactions", MIUR, Italy.

References

Bischi, G. I., Gardini, L. & Mira, C. [1999] "Maps with denominator. Part I: Some generic properties," *Int. J. Bifurcation and Chaos* **9**, 119–153.

Bischi, G. I., Gardini, L. & Mira, C. [2001] "Plane maps with a vanishing denominator. A survey of some results," *Nonlinear Analysis T.M.&A., Special Issue Proc. WCNA2000*, Vol. 47, pp. 2171–2185.

Bischi, G. I., Gardini, L. & Mira, C. [2003] "Plane maps with denominator. Part II: Noninvertible maps with simple focal points," *Int. J. Bifurcation and Chaos* **13**, 2253–2277.

Foroni, I. [2001] "Meccanismi di apprendimento in modelli omogenei ed eterogenei," PhD Thesis, University of Trieste.

Foroni, I. & Gardini, L. [2003] "Homoclinic bifurcations in heterogeneous market models," *Chaos Solit. Fract.* **15**, 743–760.

Frouzakis, C. F., Gardini, L., Kevrekidis, Y. G., Millerioux, G. & Mira, C. [1997] "On some properties of invariant sets of two-dimensional noninvertible maps," *Int. J. Bifurcation and Chaos* **7**, 1167–1194.

Gumowski, I. & Mira, C. [1980] *Dynamique Chaotique* (Cepadues Editions, Toulouse).

Mira, C., Fournier-Prunaret, D., Gardini, L., Kawakami, H. & Cathala, J. C. [1994] "Basin bifurcations of two-dimensional noninvertible maps: Fractalization of basins," *Int. J. Bifurcation and Chaos* **4**, 343–381.

Mira, C., Gardini, L., Barugola, A. & Cathala, J. C. [1996a] *Chaotic Dynamics in Two-Dimensional Noninvertible Maps* (World Scientific, Singapore).

Mira, C., Millerioux, G., Carcasses, J. P. & Gardini, L. [1996b] "Plane foliation of two-dimensional noninvertible maps," *Int. J. Bifurcation and Chaos* **6**, 1439–1462.